Dielectric anomalies and phase transition in glycinium phosphite crystal under the influence of a transverse electric field

2004 J. Phys.: Condens. Matter 16 1963

(http://iopscience.iop.org/0953-8984/16/12/006)

INSTITUTE OF PHYSICS PUBLISHING JOURNAL OF PHYSICS: CONDENSED MATTER

J. Phys.: Condens. Matter **16** (2004) 1963–1979 PII: S0953-8984(04)65867-X

Dielectric anomalies and phase transition in glycinium phosphite crystal under the influence of a transverse electric field

I Stasyuk[1,3], **Z Czapla**[2], **S Dacko**[2] **and O Velychko**[1]

[1] Institute for Condensed Matter Physics of the National Academy of Sciences of Ukraine, 1 Svientsitskii Street, 79011 Lviv, Ukraine
[2] Institute of Experimental Physics, Wrocław University, 9 M Borna Square, 50–204 Wrocław, Poland

E-mail: ista@icmp.lviv.ua

Received 8 July 2003, in final form 7 January 2004
Published 12 March 2004
Online at stacks.iop.org/JPhysCM/16/1963 (DOI: 10.1088/0953-8984/16/12/006)

Abstract

The dielectric properties of glycinium phosphite (GPI) crystals as a function of temperature and electric field magnitude are investigated. The electric field E is applied perpendicularly to the ferroelectric b-axis in the direction of hydrogen-bonded phosphite chains in the crystal (the c-axis). The shift of the paraelectric–ferroelectric phase transition to lower temperatures proportionally to E_c^2 (where E_c is an effective field in the sample) is observed. Strong anomalies in the field dependence of the permittivity ε_c' in the temperature region $T \leqslant T_c$ are revealed. It is shown that the observed jump-like changes of ε_c' are caused by the phase transition from the ferro- to paraelectric phase induced by the electric field. Such a transition is connected with the rearrangement of protons on hydrogen bonds and the reversal of the corresponding dipole moments, at which the compensation of their components along the b-axis takes place. The theoretical description of the observed dielectric anomalies, given on the basis of the phenomenological Landau free energy approach, is in good agreement with the experimental data.

(Some figures in this article are in colour only in the electronic version)

1. Introduction

Glycinium phosphite (abbreviated as GPI) belongs to the hydrogen-bonded family of ferroelectric crystals [1, 2]. At room temperature it crystallizes in a monoclinic system with a space group $P2_1/a$ [3]. In the crystal structure one can distinguish infinite chains

[3] Author to whom any correspondence should be addressed.

of hydrogen-bonded PO_3H tetrahedra parallel to the crystallographic c-axis. There are two types of hydrogen bond of lengths ∼2.48 and ∼2.52 Å with protons disordered between two equilibrium positions in the double potential wells [3–5]. Ordering of protons in these hydrogen bonds [4, 5] leads to antiparallel polarization along the a- and c-axes in particular chains. At the same time, the changes of some distances between ions in HPO_3 tetrahedra, and the addition of components of dipole moments connected with hydrogen bonds, produce a nonzero dipole moment along the b-axis which becomes a ferroelectric one below 225 K. The space group of this phase is $P2_1$; spontaneous polarization is perpendicular to the direction of chains of hydrogen bonds. Thus, interactions in the chains, as well as long-range dipolar interactions, are generally involved in the mechanism of phase transition.

The physical properties of the GPI crystal have been studied in a number of works. The influence of deuteration on T_c was investigated; the results of experiments give strong support to the proton ordering mechanism of the phase transition and point out the important role of hydrogen bonds. The isotope effect is significant: the phase transition point shifts considerably to higher temperatures ($T_c^D - T_c^H = 97$ K [6]). The dependence of T_c on deuterium content is linear [7]. Besides the large shift in T_c, one can mention the 'geometric' isotope effect (a linear change of the R_{0-0} distance in hydrogen bonds at deuteration of the crystal). There is a direct correlation between ΔR_{0-0} and ΔT_c for partially deuterated GPI crystals [8], very similar to that for a variety of H-bonded ferroelectrics with phase transitions caused by the ordering of protons.

The measurement of electric permittivity along the b-axis was performed. The temperature behaviour of the ε_b component as well as the spontaneous polarization $\boldsymbol{P}_s$ was studied; the conclusion was made that the phase transition is of second order and can be regarded as being close to a tricritical one [9]. A significant anomaly of permittivity in the c-direction was also detected; at room temperature ε_c is higher than ε_b [1].

One should mention also the high hydrostatic pressure studies of the transition into the ferroelectric phase in GPI. The effect of pressure is significant. With increase of pressure, T_c decreases with $dT_c/dp = -11.0$ K kbar^{-1} [10]. Such a decrease is of the same order as values of dT_c/dp for other ferroelectrics with ordering of protons on hydrogen bonds.

Besides structure investigations, the measurement of the frequency dependence of electric permittivity also leads us to the conclusion that the phase transition in GPI is of the order-disorder type [11, 12]. However, reorientation and deformation of the ionic group (phosphite anions) could also play an important role (the corresponding structure changes can be extracted from the neutron scattering data [5]). The observed temperature anomalies of elastic constants in the vicinity of T_c [13] were explained as a manifestation of the probably pseudo-proper origin of ferroelectricity in GPI due to anharmonic interaction of the order parameter with deformation of the crystal lattice.

Although from the present experimental data conclusions can be made about the significant role of hydrogen bonds and ordering of protons in the appearance of the ferroelectric phase in the GPI crystal, the microscopic description of the transition into this state is still in development. To obtain a more clear understanding of the problem, and to obtain information on the phase transition in GPI, we decided to study the dielectric properties of the crystal under the influence of the electric field acting in the c-direction parallel to the H-bonded chains. Such a field being applied perpendicularly to the ferroelectric axis is not conjugated to the order parameter (polarization $\boldsymbol{P}_s \parallel \boldsymbol{b}$) relevant for the phase transition. Our study is supplemented by the microscopic consideration, based on recently obtained information about the changes in the structure (including the changes in distribution of protons on hydrogen bonds) at the paraelectric–ferroelectric phase transition [4, 5]. A symmetry analysis of the microscopic order parameters is performed. Starting from the obtained data, the approach based on the

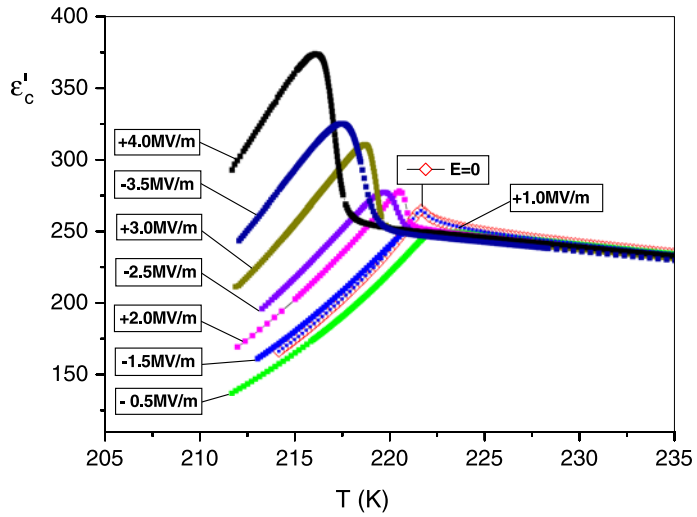

Figure 1. Temperature dependences of permittivity ε_c' for various values of dc electric field E.

phenomenological Landau expansion is used. The phase transition into the ferroelectric phase in the presence of an external electric field E ($\boldsymbol{E} \parallel \boldsymbol{c}$) is described. Attention is paid to the shift of the transition temperature and to the changes in the behaviour of the electric permittivity ε_c'. The experimentally observed anomalies in temperature and field dependences of ε_c' are described. A possible microscopic mechanism responsible for the revealed field effects is discussed.

2. Experimental details

Single crystals of GPI were grown from saturated water solution of recrystallized polycrystals of the substance by a slow evaporation method at a temperature of 304 K. The c-plates of thickness about 0.25 mm were cut out from a large crystal. Silver paste was used as electrodes. The capacity of the samples was measured with a precise LCR-meter HP 4284 A. The measuring field frequency was equal to 10 kHz with an amplitude of 400 V m^{-1}. Relative electric permittivity ε_c' in the direction of the c-axis was measured as a function of temperature with various values of dc electric field E ranging from zero to 4 MV m^{-1} and acting in the same direction. The measurement was done during cooling with the rate of temperature change equal to 0.5 K min^{-1}.

At constant temperature a slowly changing sinusoidal electric field of amplitude 4 MV m^{-1} and frequency of 10^{-2} Hz was applied to the sample. Evaluations of permittivity were performed by measurements of capacity done with the help of the simultaneously applied probing field from the HP 4284 LCR-meter at the frequency 10 kHz and amplitude of measuring field 400 V m^{-1}. The temperature of the samples was stabilized with accuracy not worse than 5×10^{-3} K.

2.1. Temperature dependences of permittivity for various values of dc electric field

Temperature dependences of relative electric permittivity ε_c' measured at various values of dc field E are presented in figure 1.

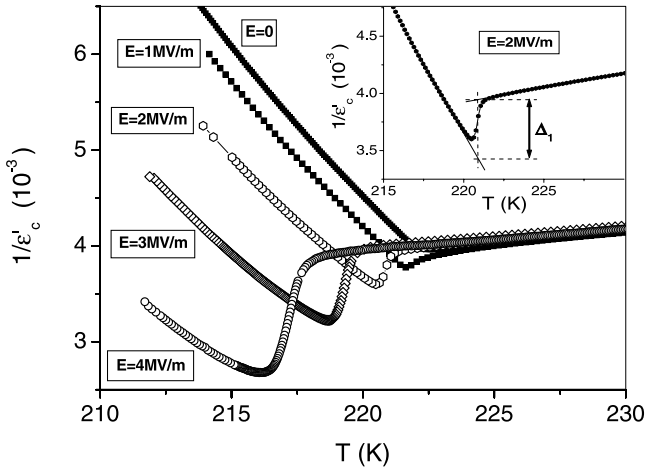

Figure 2. Temperature dependences of inverse permittivity for various values of dc electric field E. The inset demonstrates the jump Δ_1 of inverse permittivity at the phase transition.

Similarly to the previous measurement at zero applied field [1] the large value of permittivity is observed at room temperature. During the cooling run we observe an increase of permittivity. In the vicinity of the phase transition point, as can be seen in figure 1, a strong increase of permittivity at lowering of temperature takes place. The peak becomes higher and its position is shifted to lower temperatures with an increase of the electric field magnitude. On further cooling a decrease of permittivity is observed.

The inverse permittivity as a function of temperature is shown in figure 2. Besides the transition region the Curie–Weiss law is fulfilled with different slopes both in paraphase and below the phase transition temperature. In the vicinity of T_c a smooth jump-like change of $1/\varepsilon'_c$ is observed. Though the observed anomalies of ε'_c and $1/\varepsilon'_c$ functions are rather continuous, we approximate them by jump-like dependences supposing that we are dealing with the partially diffused transition. As the temperature of the phase transition we assume the middle point of the interval in which the transition from one straight line for $1/\varepsilon'_c$ in paraphase to another, representing its strong increase in the low temperature phase (see an inset in figure 2), takes place. This experiment shift of the phase transition temperature under the influence of the electric field E_c observed (see below) is presented in figure 3.

If we interpret the change of permittivity in the vicinity of T_c under the field as a jump-like increase we can represent its value as a 'jump' of $1/\varepsilon'_c$ defined as Δ_1. Without field Δ_1 is equal to zero. The observed jump depends on the total value of electric field acting in the sample.

If we assume the existence of an internal bias field E_{bias} and introduce the effective field E_c ($E_c = E - E_{\text{bias}}$ or $-E - E_{\text{bias}}$ depending on the direction of the applied field E), we can notice that the value of this jump increases linearly with $(\pm E - E_{\text{bias}})^2$ as illustrated in figure 4. It is worth noting that the E_{bias} value is small in comparison with the value of applied fields. Without E_{bias} the experimental points would be placed on two parallel straight lines (for $+E$ and for $-E$).

2.2. Field dependences of permittivity at constant temperature

2.2.1. Paraelectric phase. The electric permittivity ε'_c measured as the function of electric field E for the chosen temperature of 230.9 K in the paraelectric phase is presented in figure 5.

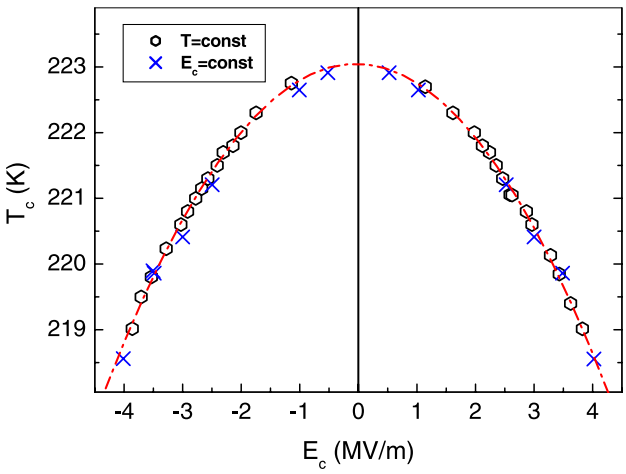

Figure 3. The dependence of T_c on E_c: ×—obtained from the temperature dependence of permittivity at constant electric field, ⬡—obtained from the field dependence of electric permittivity at constant temperature.

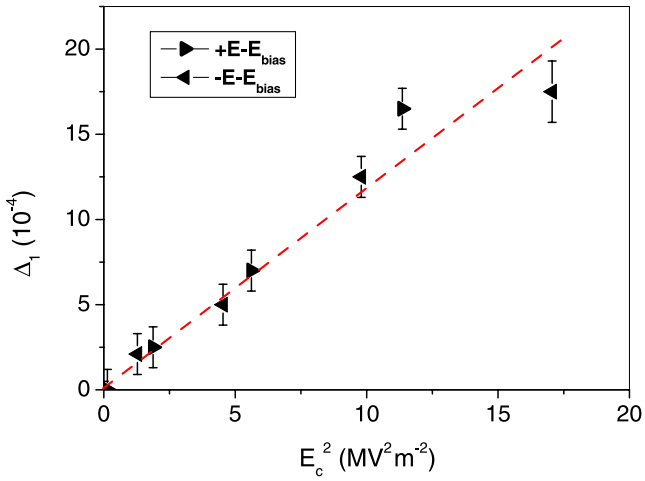

Figure 4. The jump Δ_1 of inverse permittivity as a function of E_c^2.

As can be seen, the permittivity increases a little and a broad maximum of its value is observed at about 1.0 MV m^{-1}; next a clear decrease of permittivity takes place. At the decrease of electric field a nearly linear increase of permittivity is observed and the initial value is reached at the field equal to zero. The change of electric field in the opposite direction gives a practically symmetric dependence. Thus one can see the hysteresis behaviour of permittivity as a function of the electric field magnitude. We assumed that such a behaviour can be caused by the internal field changing its value with the same frequency as the frequency of the applied field but shifted in phase. The space charges redistributing in the bulk [14], and polarization related to defects [15] in the crystal under the influence of the field E, can be the source of such an internal field. A similar effect was revealed previously in deuterated CsH_2PO_4 crystal [16]. To compensate for this effect we introduce formally the correction field E_{corr} fitting in calculating

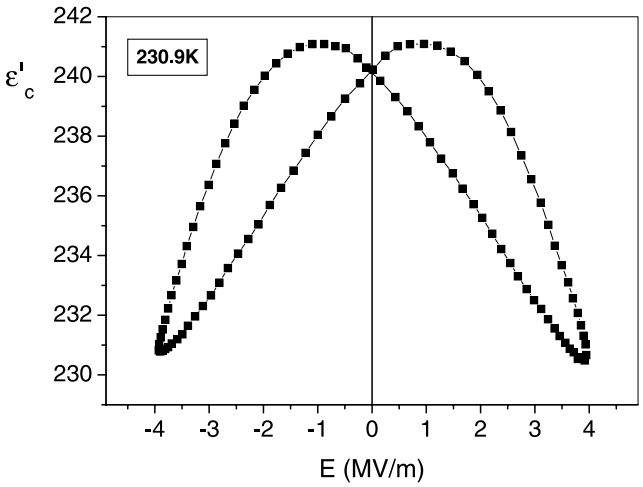

Figure 5. The electric permittivity ε_c' as a function of the electric field applied in the c-axis direction at 230.9 K.

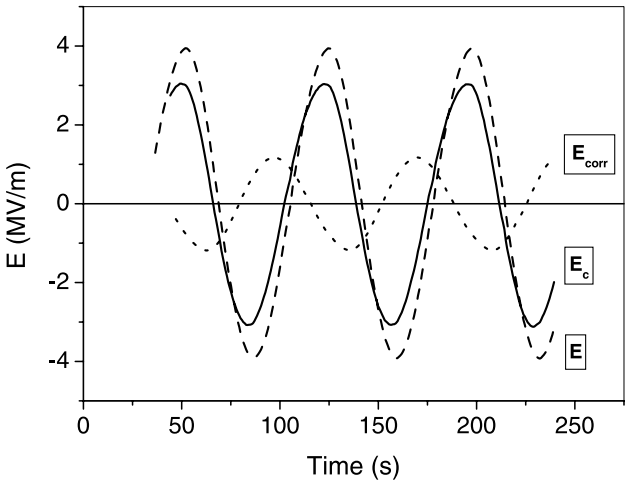

Figure 6. The time dependences of applied, internal and effective electric fields acting in the sample.

its amplitude and phase in such a way that hysteresis is maximally eliminated; it is supposed that the difference in both fields has the same meaning as the above-mentioned effective field in the static case: $E - E_{\rm corr} = E_c$ (see figure 6).

Using the effective field we can see that the maximum value of permittivity is reached at zero field (as expected, figure 7(a)). We could not remove the hysteresis totally, but we can represent the dependence of permittivity versus the electric field E_c at small enough field as a quadratic function (figure 7(b)).

Generally, over the whole temperature range in the paraelectric phase the behaviour of permittivity with electric field magnitude is quite similar. One can notice that in this phase the changes of permittivity are relatively small (about 4%). These changes become larger at lower temperatures and the hysteresis becomes much smaller.

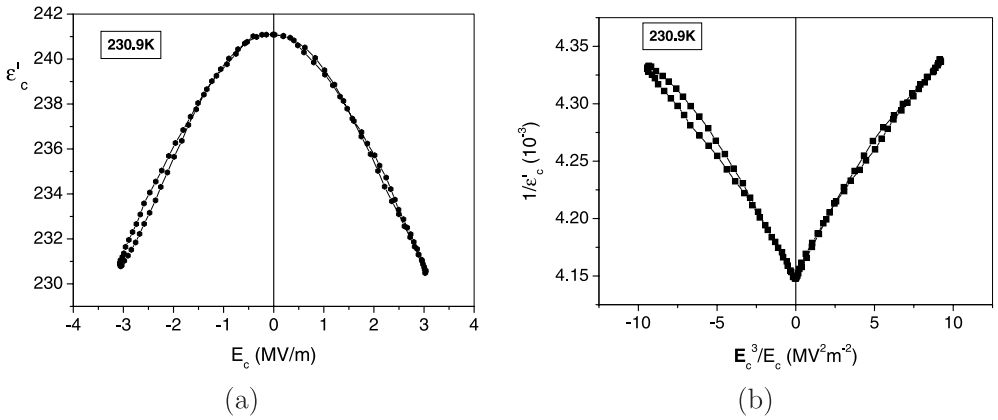

Figure 7. Electric permittivity ε_c' as a function of $E_c = E - E_{\rm corr}$ (a) and inverse electric permittivity $1/\varepsilon_c'$ versus $(E - E_{\rm corr})^2$ (b) at 230.9 K.

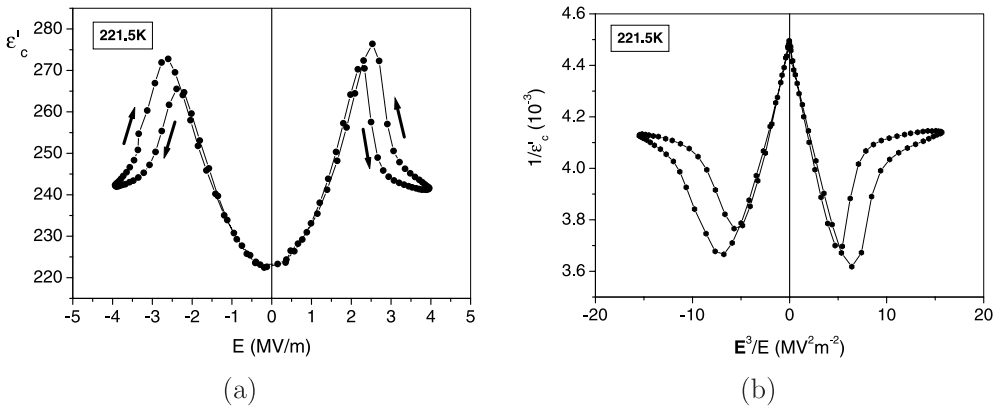

Figure 8. Electric permittivity ε_c' as a function of the electric field (a) and inverse electric permittivity $1/\varepsilon_c'$ versus E^2 (b) measured at 221.5 K.

2.2.2. Ferroelectric phase. The relative electric permittivity ε_c' as a function of the electric field E (range 0–4 MV m^{-1}) was measured in the vicinity of the phase transition in the temperature range $T_{\rm c} - 4.5$ K $< T < T_{\rm c}$ and the results obtained at 221.5 K are presented in figure 8(a).

As can be seen in figure 8(a), we observe an increase of permittivity with the increase of the electric field magnitude in the range of ± 2.5 MV m^{-1}. Near these values of electric field the permittivity reached its maximum for both directions of the electric field. On further increase of the electric field a strong decrease of permittivity is observed in some range of applied fields and after that the next increase of electric field gives a weak decrease of permittivity. We can interpret an appearance of maximum and such a sharp change as a transition from ferroelectric to paraelectric phase caused by the electric field (see figure 3). While the increase of permittivity with the field E is characteristic of the ferroelectric phase, a sharp decrease of permittivity takes place when the paraelectric phase is achieved. On further increase of the electric field the permittivity decreases; the observed changes of ε_c' are small (similar to the behaviour of ε_c' seen in figure 7(a)). The results from figure 8(a) can also be presented as the $1/\varepsilon_c'$ versus E^2

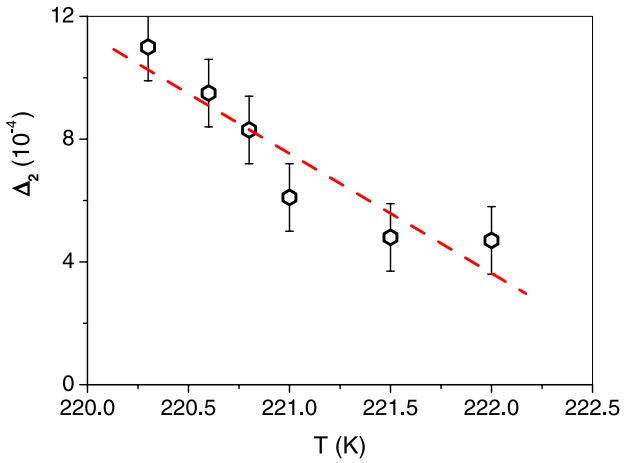

Figure 9. The jump Δ_2 of inverse permittivity as a function of temperature.

dependence as is shown in figure 8(b). We consider this dependence in the range 0–4 MV^2 m^{-2} to be a linear one. In the range 4–6 MV^2 m^{-2} a strong increase of $1/\varepsilon_c'$ is observed. We can treat it as a jump defined as Δ_2 (see below). In the range 6–10 MV^2 m^{-2}, the dependence of $1/\varepsilon_c'$ again becomes nearly linear with a low slope. In our measurement we observed hysteresis in the region of rapid changes of permittivity or $1/\varepsilon_c'$, as can be seen in figures 8(a) and (b). At the chosen temperature of 221.5 K the phase transition point T_c is achieved at the field magnitude equal to 2.5 MV m^{-1} (increase of the field) and equal to 2.2 MV m^{-1} (decrease of the field). In the region of the small field values the observed hysteresis at $T < T_c$ is much smaller in comparison with the behaviour of ε_c' in the paraelectric phase. It allows us to neglect the difference between field E and the effective field E_c in this case.

The obtained dependence of Δ_2 on temperature is presented in figure 9 (similar to the case of the Δ_1 parameter, Δ_2 is defined as a jump from one to another linear dependence $1/\varepsilon_c'$ on E_c^2 in the middle point of the above-mentioned transition region of the electric field). The dependence of the phase transition temperature on the electric field, taken from the measurements of ε_c' at different (but constant) temperatures with the change of electric field E applied to the sample, is in very good agreement with data obtained from the temperature dependences of ε_c' at different fields (see figure 3).

Results of measurements done in the ferroelectric phase at 211.3 K are presented in figure 10(a). The observed dependence ε_c' on E shows a strong increase of permittivity with the increase of the electric field. In the range of the field (0–4 MV m^{-1}), only an increase of permittivity is observed.

In figure 10(b) $1/\varepsilon_c'$ found in experiments at 211.3 K is also presented as a function of E^2. One can approximate this dependence as a linear one. We can see here only a decrease of $1/\varepsilon_c'$ and this means that in the whole range of applied fields we are always in the ferroelectric phase. One should mention here that the results of the measurements at different temperatures in the ferroelectric phase far below T_c are quite similar.

3. Proton ordering and order parameters

In order to understand the experimentally observed effect caused by the electric field E_c acting perpendicularly to the ferroelectric axis, we shall discuss the question of the influence of such a field on the proton subsystem of GPI. If the phase transition in GPI is supposed to be connected

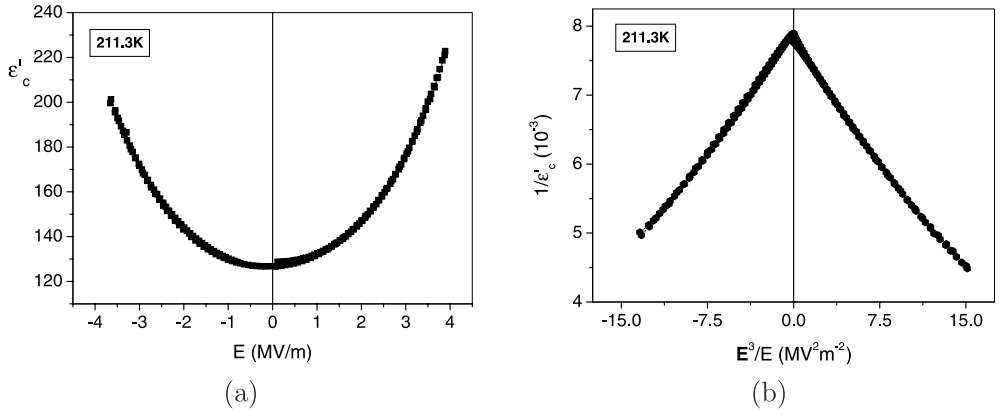

Figure 10. Field dependence of electric permittivity as a function of E (a) and inverse electric permittivity $1/\varepsilon_c'$ as function of E^2 (b) at 211.3 K.

with ordering of protons on hydrogen bonds, the revealed dielectric anomalies and changes in the picture of the phase transition should be related to the changes in distribution of protons. The microscopic model of the phase transition in GPI based on this assumption is developed elsewhere [17]. Here, we consider only some structural aspects and discuss the result of the symmetry analysis.

We start from the structural data for localization of hydrogen bonds and equilibrium positions of protons in the paraelectric and ferroelectric phases [4, 5]. In the unit cell of the crystal there are four translationally nonequivalent bonds (the 011–021 and 013–023 bonds in notations used in [4] and also another two connected with the ones mentioned by point symmetry operations). Their projections on the XZ and YZ planes are shown in figures 11(a) and (b) (the Cartesian Y and Z axes coincide with the crystallographic axes b and c, respectively; the Cartesian X- (or a'-) axis makes an angle of 100.43° with the crystallographic c-axis in the (a, c) plane). Directions connected with the ordering of protons and corresponding to the prevailing occupancy of proton positions in the ferroelectric phase ($n_{i1} > n_{i2}$, where $n_{i\alpha}$ is the proton occupation number in the α position ($\alpha = 1, 2$) on the i bond) are shown by arrows.

As can be seen, the dipole moments $\boldsymbol{d}_i$ connected with protons on bonds compensate mutually in pairs ($\boldsymbol{d}_1$ and $\boldsymbol{d}_3$; $\boldsymbol{d}_2$ and $\boldsymbol{d}_4$) in the low temperature phase in the Z and X directions. At the same time, they sum up along the Y-axis leading to the appearance of spontaneous polarization. Thus, we have the situation with ferroelectric type ordering, when the ferroelectricity along the b-axis is accompanied by the antiferroelectric-like (antiparallel) arrangement of dipole moments of the neighbouring H-bonded chains (A and B chains in figure 11) along the c-axis (the chains are oriented in this direction).

According to data given in [4], in the fully ordered state

$$\begin{aligned} &\boldsymbol{d}_1 = (-a, -b, -c), \qquad \boldsymbol{d}_2 = (d, e, -f), \\ &\boldsymbol{d}_3 = (a, -b, c), \qquad \boldsymbol{d}_4 = (-d, e, f), \end{aligned} \tag{3.1}$$

where

$$\begin{aligned} &a = 0.239q, \qquad b = 2.361q, \qquad c = 0.786q, \\ &d = 1.221q, \qquad e = 1.279q, \qquad f = 1.568q. \end{aligned} \tag{3.2}$$

The numerical coefficients are given in ångströms; q is an effective charge connected with proton on the bond. To describe the proton ordering we use the variables $S_0^Z = \frac{1}{2}(n_{i1} - n_{i2})$

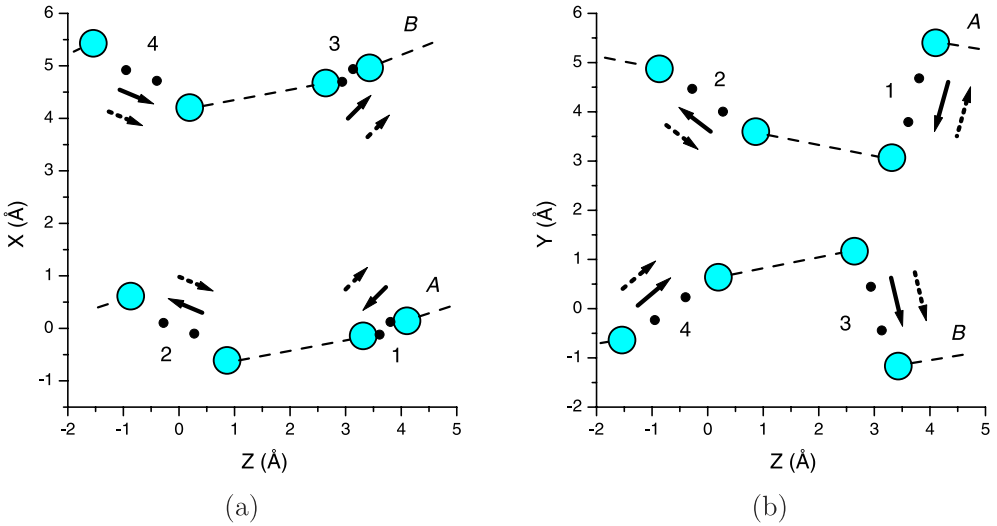

Figure 11. Equilibrium position of H-atoms on hydrogen bonds in the unit cell of the GPI crystal in the paraphase (the directions of dipole moments connected with the ordering of protons are shown by solid arrows in the ferroelectric phase F and by dashed ones in the state with $\boldsymbol{P} \parallel OZ$—the phase F'): (a) projection on the XZ ($a'c$) plane; (b) projection on the YZ (bc) plane.

and introduce the dipole moments $\hat{D}_i^\alpha = d_i^\alpha S_i^Z$. In the absence of the external field the mean values $\eta_i = \langle S_i^Z \rangle$ are equal to zero in the paraphase ($\eta_1 = \eta_2 = \eta_3 = \eta_4 = 0$) while in the ferroelectric phase with polarization along the b-axis they are $\eta_1 = \eta_3 \neq 0$ and $\eta_2 = \eta_4 \neq 0$.

Using four self-consistency parameters η_k ($k = 1, \ldots, 4$), responsible for the proton orderings, one can construct the quantities

$$D^y_{A(B)} = -b\eta_{1(3)} + e\eta_{2(4)}, \qquad D^z_{A(B)} = \mp c\eta_{1(3)} \mp f\eta_{2(4)}, \tag{3.3}$$

describing contributions to the polarization of the crystal along the b- and c-axes, respectively. Their sums and differences (when the polarizations of chains of the A and B type are combined) create, by means of the linear combination, the order parameters

$$\left.\begin{matrix} D^y_A + D^y_B \\ D^z_A - D^z_B \end{matrix}\right\} \to \eta_b, \qquad \left.\begin{matrix} D^y_A - D^y_B \\ D^z_A + D^z_B \end{matrix}\right\} \to \eta_c \tag{3.4}$$

(see for details [17]).

The parameter η_b transforms according to the irreducible representation A_u of the group C_{2h} (which is the point symmetry group of the paraphase) and describes both ferroelectric ordering of protons along the b-axis and the antiferroelectric one along the c-axis (see figure 11). The parameter η_c belongs to the representation B_u and is responsible for antiferroelectric ordering along the b-axis and for ferroelectric type ordering (with the nonzero component of the total dipole moment) along the c-axis. The state with $\eta_b \neq 0$, $\eta_c = 0$ corresponds to the phase F which realizes below T_c in GPI, while the state with $\eta_b = 0$, $\eta_c \neq 0$ describes the phase F' with spontaneous ferroelectric ordering along the c direction. We suppose (see below) that the phase F' could probably appear spontaneously in GPI at low temperatures in the absence of the transition into the phase F. It should be mentioned in this connection that it is known as an example of the phase transition with the replacement of directions of ferroelectric and antiferroelectric ordering: one can mention here the DMAGaS crystal [18].

When the field E_c is present and the polarization component along the Z-axis appears under its influence, the above-mentioned relations break down and $\eta_1 \neq \eta_3$, $\eta_2 \neq \eta_4$.

In this case, in the paraelectric phase $\eta_3 = -\eta_1$, $\eta_4 = -\eta_2$, while in the ferroelectric phase $\eta_3 \neq -\eta_1$, $\eta_4 \neq -\eta_2$. The phase transition, observed in the GPI crystal under the influence of electric field at $T \lesssim T_c^0$, where T_c^0 is the temperature of transition at the zero field, is a transition at which the crystal transforms from the initial state with $\boldsymbol{P}_s \parallel OY$ (at $E_c = 0$) into the state with $\boldsymbol{P} \parallel OZ$ (at large enough values of E_c). It is accompanied by the reversal of dipole moments connected with hydrogen bonds on the H-bonded chains of one of two types (see figure 11). The induced by field redistribution of protons leads to the compensation of dipole moments along the b-axis and to their addition along the c-axis. Such an ordering is characteristic of the phase F', but appears here as the induced (not spontaneous) one.

The arguments presented above give an explanation of the experimentally observed decrease of temperature of the transition into the ferroelectric phase under the field E_c. Indeed, due to the special orientation of hydrogen bonds in the crystal (at certain angles with the crystallographic axes) the field E_c, favouring the orientation of the hydrogen bond dipoles shown by dashed arrows in figure 11, counteracts at the same time their ordering with the total moment parallel to the b-axis (solid arrows in figure 11).

4. The Landau expansion

We use here a phenomenological description based on the Landau free energy expansion in order to investigate theoretically the behaviour of the transverse susceptibility χ_{zz} and, respectively, the electric permittivity $\varepsilon_c' = 1 + \chi_{zz}$ in the presence of the field $E_z \equiv E_c$ (at the exclusion of effects connected with the influence of the above-mentioned bias or internal fields the field E_c plays the role of the acting field in such an expansion).

Let us express the Landau free energy in terms of order parameters η_b and η_c. We present it in the form

$$F = F_0 + \tfrac{1}{2}a\eta_b^2 + \tfrac{1}{2}b\eta_c^2 + \tfrac{1}{4}c\eta_b^4 + \tfrac{1}{4}d\eta_c^4 + \tfrac{1}{2}f\eta_b^2\eta_c^2 + \left(\tfrac{1}{6}g\eta_c^6 + \text{other terms of the 6th order}\right) - E_c\eta_c, \tag{4.1}$$

where the energy in the effective field acting in the c direction is included.

In the case of the second order phase transition into the phase F

$$a = a'(T - T_c^0), \qquad a' > 0, \quad c > 0. \tag{4.2}$$

The temperature dependence of the b coefficient is also taken into account

$$b = b'(T - T^*), \qquad b' > 0. \tag{4.3}$$

Here T^* (while $T^* < T_c^0$) is the temperature of the 'virtual' transition of the second order from the paraphase into the phase F' (see the previous section).

A standard analysis based on the equilibrium conditions

$$\frac{\partial F}{\partial \eta_b} = 0, \qquad \frac{\partial F}{\partial \eta_c} = 0 \tag{4.4}$$

shows that the temperature of the transition into the phase F decreases under influence of the field

$$T_c = T_c^0 - \frac{f}{a'b_0^2}E_c^2 \tag{4.5}$$

proportional to E_c^2; here $b_0 = b'(T_c^0 - T^*)$. The effect takes place at $f > 0$ and is the consequence of the bilinear interaction between the polarization components along the b- and c-axes.

The order parameter η_b is determined in the phase F from the equation

$$a + c\eta_b^2 + f\eta_c^2 = 0. \tag{4.6}$$

As a result, the renormalization

$$b \to \tilde{b} = b - af/c, \qquad d \to \tilde{d} = d - f^2/c \tag{4.7}$$

takes place in the expansion in terms of the parameter η_c.

Let us consider now the case $d > 0$, $\tilde{d} < 0$. In such a situation the transition into the phase F' could be realized (if it were possible) from the phase F at temperature T_1 which is obtained from the equation

$$16\tilde{b}g = \tilde{d}^{\,2}, \tag{4.8}$$

as in the case of the phase transition of the first order. At the fulfilment of the condition $T^* < T_1 < T_c$, the phase F' does not appear (the case of GPI crystal) and only the transition into the phase F exists. The transition is of second order at $E_c = 0$ in this case; it can be shown (see appendix for details) that the order of the transition does not change at $E_c \neq 0$ at least in the region of not too strong fields.

Starting from equilibrium conditions (4.4) one can find the susceptibility $\tilde{\chi}_{zz} = \varepsilon_0 \chi_{zz}$ which is defined in the model by the derivative $\partial\eta_c/\partial E_c$:

$$\tilde{\chi}_{zz} = \frac{\partial \eta_c}{\partial E_c}, \tag{4.9}$$

where ε_0 is the electric permittivity of vacuum. Up to terms of second order in E_c

$$\frac{\partial \eta_c}{\partial E_c} = \frac{1}{b} - \frac{3d}{b^4}E_c^2, \qquad T > T_c, \tag{4.10a}$$

$$\frac{\partial \eta_c}{\partial E_c} = \frac{1}{\tilde{b}} + \frac{3|\tilde{d}|}{\tilde{b}^4}E_c^2, \qquad T < T_c. \tag{4.10b}$$

In the considered case the susceptibility $\tilde{\chi}_{zz}$ decreases with field in the paraphase ($T > T_c$) and increases in the ferroelectric phase ($T < T_c$), proportionally to E_c^2 in both cases.

The temperature dependences of $\tilde{\chi}_{zz}$ at $E_c = 0$ are given by the expressions

$$\tilde{\chi}_{zz} = \frac{1}{b'(T - T^*)}, \qquad T > T_c, \tag{4.11a}$$

$$\tilde{\chi}_{zz} = \left[\left(b' - \frac{a'f}{c}\right)T + \frac{a'f}{c}T_c^0 - b'T^*\right]^{-1}, \qquad T < T_c. \tag{4.11b}$$

In the case of the paraphase the susceptibility $\tilde{\chi}_{zz}$ increases at the lowering of temperature (due to the condition $b' > 0$). In the ferroelectric phase the temperature dependence of $\tilde{\chi}_{zz}$ is of the opposite character at $b' < a'f/c$.

The inverse susceptibility $\tilde{\chi}_{zz}^{-1}$ in our approximation is a linear function of temperature with slope b' in the paraphase and $b' - a'f/c$ in the ferroelectric phase. At $E_c \neq 0$

$$\tilde{\chi}_{zz}^{-1} = b'(T - T^*) + \frac{3d}{[b'(T - T^*)]^2}E_c^2, \qquad T > T_c, \tag{4.12a}$$

$$\tilde{\chi}_{zz}^{-1} = \left(b' - \frac{a'f}{c}\right)T + \frac{a'f}{c}T_c^0 - b'T^* - \frac{3|\tilde{d}|}{\tilde{b}^2}E_c^2, \qquad T < T_c. \tag{4.12b}$$

At the point of the paraelectric–ferroelectric phase transition, at $E_c = 0$

$$\tilde{\chi}_{zz}|_{T=T_c} = \frac{1}{b_0}, \tag{4.13}$$

while at $E_c \neq 0$

$$\tilde{\chi}_{zz}|_{T=T_c+0} = \frac{1}{b_0} - \frac{3d - b'f/a'}{b_0^4} E_c^2 \tag{4.14}$$

from the paraelectric phase side, and

$$\tilde{\chi}_{zz}|_{T=T_c-0} = \frac{1}{b_0} - \frac{3d - b'f/a' - 2f^2/c}{b_0^4} E_c^2 \tag{4.15}$$

from the ferroelectric side. There exists a jump of $\tilde{\chi}_{zz}$ and, respectively, of $\tilde{\chi}_{zz}^{-1}$ in the transition point at $E_c \neq 0$. Its magnitude is proportional to E_c^2:

$$\tilde{\Delta}_1 \equiv \tilde{\chi}_{zz}^{-1}\big|_{T=T_c+0} - \tilde{\chi}_{zz}^{-1}\big|_{T=T_c-0} = \frac{2f^2}{cb_0^2} E_c^2. \tag{4.16}$$

The jump-like behaviour of χ_{zz} is not in contradiction to the second order nature of the phase transition at T_c. The susceptibility χ_{zz} describes the crystal response with respect to the field acting perpendicularly to the ferroelectric b-axis. The susceptibility χ_{yy} in the direction of this axis is still divergent (see appendix).

We would like to point out that the temperature behaviour of the susceptibility $\tilde{\chi}_{zz}$ at fixed field E_c values is the same as was predicted for the dielectric susceptibility of the uniaxial antiferroelectric along the antipolarization direction under the longitudinal field (see [15], as well as citations herein). The expansion (4.1) used by us in terms of two interacting order parameters is analogous to the one applied in that case. The results of the analysis presented in [15] show that the induced field transition from the antipolar phase to the polar one is of second order at field values not exceeding some critical value (when the smaller value of χ_{zz}^{-1} at the jump point remains positive, decreasing in its magnitude with an increase of the field).

Let us return to the field dependences of susceptibility $\tilde{\chi}_{zz}$. It is possible (due to the decrease of T_c with the field) that starting at $T \leqslant T_c$ from the ferroelectric phase, we will cross the phase transition line at a certain field E_c^* ($E_c^* = b_0[(a'/f)(T_c^0 - T)]^{\frac{1}{2}}$) and pass to the paraelectric phase. In such a case the $\tilde{\chi}_{zz}(E_c)$ dependence of the (4.10*b*) type, being described by an increasing function of field, will change into a decreasing function (4.10*a*). At the transition point the $\tilde{\chi}_{zz}(E_c)$ function jumps down; respectively, the inverse susceptibility goes up:

$$\tilde{\Delta}_2 \equiv \tilde{\chi}_{zz}^{-1}\Big|_{E_c^*+0} - \tilde{\chi}_{zz}^{-1}\Big|_{E_c^*-0} = \frac{2a'f}{c}(T_c^0 - T). \tag{4.17}$$

The jump magnitude is connected linearly with the deviation of the given temperature from the temperature T_c^0 of the phase transition in the absence of field E_c.

The temperature and field dependences of $\tilde{\chi}_{zz}$ and $\tilde{\chi}_{zz}^{-1}$ discussed above are in direct correspondence with the those obtained experimentally and illustrated in figures 1, 2, 8(a), (b), etc. It is possible to make a qualitative comparison and to check the validity of the Landau expansion approach in the description of the observed dielectric anomalies (see the next section).

5. Numerical estimates

The phenomenological approach developed in the previous section gives in general a qualitative description of the measured dielectric anomalies along the c-axis when the external electric field $\boldsymbol{E} \parallel \boldsymbol{c}$ is applied. The more detailed comparison of the calculated and experimental temperature and field dependences of dielectric permittivity ε_c' enables us to make the corresponding numerical estimates.

Using the experimental data (figure 2) for the slope of the curves $\varepsilon_c'^{-1}(T)$ at $T > T_c$, which is determined due to the relation $\varepsilon_c' \approx \tilde{\chi}_{zz}/\varepsilon_0$ by the coefficient $\varepsilon_0 b'$, we obtain

$$\varepsilon_0 b' = 2.35 \times 10^{-5}\ \mathrm{K}^{-1} \tag{5.1}$$

(the given value is a result of an averaging procedure for curves $\varepsilon_c'^{-1}$ measured at different field magnitudes). Taking into account that the experimental value of $\varepsilon_c'^{-1}|_{E_c=0} = \varepsilon_0 b'(T - T^*)$ at $T = 230.9$ K (figure 2) is $\varepsilon_c'^{-1} = 41.7 \times 10^{-4}$, we have

$$T^* = 53.5\ \mathrm{K}. \tag{5.2}$$

The data for the field dependences of $\varepsilon_c'^{-1}$ at $T > T_c$ allow us to estimate the ratio $3d/b^2$. At $T = 230.9$ K (figure 7(b)) $3\varepsilon_0 d/b^2 = (1.6{-}1.8) \times 10^{-5}$ $(\mathrm{m/MV})^2$, $\varepsilon_0 b = 41.7 \times 10^{-4}$; so we have for the coefficient d:

$$\varepsilon_0 d = 11.8 \times 10^{11}\ (\mathrm{m/MV})^2\ (\mathrm{m/F})^2. \tag{5.3}$$

From the other side, a similar procedure, performed for the curves $\varepsilon_c'^{-1}(T)$ at $T < T_c$, can be used in the estimation of parameters entering into an expression for the renormalized coefficient $\tilde{b}$:

$$\tilde{b} = \left(b' - \frac{a'f}{c}\right) T + \frac{a'f}{c} T_c^0 - b'T^*. \tag{5.4}$$

It is obtained that (figure 2)

$$\varepsilon_0 \left(b' - \frac{a'f}{c}\right) = -2.18 \times 10^{-4}\ \mathrm{K}^{-1}, \qquad \varepsilon_0 \left(\frac{a'f}{c} T_c^0 - b'T^*\right) = 52.7 \times 10^{-3} \tag{5.5}$$

and, from comparison with (5.1),

$$\frac{\varepsilon_0 a' f}{c} = 2.42 \times 10^{-4}\ \mathrm{K}^{-1}. \tag{5.6}$$

With the help of the measured field dependences of ε_c' in the ferroelectric phase, and using the relation $\varepsilon_c'^{-1} = \varepsilon_0 \tilde{b} + (3\varepsilon_0 \tilde{d}/\tilde{b}^2) E_c^2$, we can estimate the ratio $3\tilde{d}/\tilde{b}^2$ and, separately, the $\tilde{b}$ and $\tilde{d}$ coefficients. At $T = 221.5$ K (see figure 8(b))

$$\frac{3\varepsilon_0 \tilde{d}}{\tilde{b}^2} = -1.68 \times 10^{-4}\ (\mathrm{m/MV})^2, \qquad \varepsilon_0 \tilde{d} = -12.0 \times 10^{12}\ (\mathrm{m/MV})^2\ (\mathrm{m/F})^2,$$
$$\varepsilon_0 \tilde{b} = 41.0 \times 10^{-4}. \tag{5.7}$$

At the decrease of temperature the values of the $3\tilde{d}/\tilde{b}^2$ and $\tilde{d}$ quantities increase (at $T = 218.4$ K, $3\varepsilon_0 \tilde{d}/\tilde{b}^2 = -2.3 \times 10^{-4}$ $(\mathrm{m/MV})^2$, $\varepsilon_0 \tilde{d} = -24.6 \times 10^{12}$ $(\mathrm{m/MV})^2$ $(\mathrm{m/F})^2$).

Using the definition (4.7) we estimate the ratio $\varepsilon_0 f^2/c$ at temperatures near T_c:

$$\frac{\varepsilon_0 f^2}{c} = 13.3 \times 10^{12}\ (\mathrm{m/MV})^2\ (\mathrm{m/F})^2 \tag{5.8}$$

and because (see figure 2)

$$\varepsilon_0 b_0 \equiv \varepsilon_0 b|_{T=T_c^0} = 39.6 \times 10^{-4}, \qquad b_0 = 4.47 \times 10^8\ \mathrm{m/F} \tag{5.9}$$

at $T_c^0 = 222.2$ K, we have

$$\frac{\varepsilon_0 f^2}{c b_0^2} = 6.64 \times 10^{-5}\ (\mathrm{m/MV})^2. \tag{5.10}$$

Such a value is in a good agreement with the value of the coefficient at E_c^2 in the expression for the jump Δ_1 of inverse permittivity $\varepsilon_c'^{-1}$ on their temperature dependence at the given field magnitude ($\Delta_1 = \varepsilon_0 \tilde{\Delta}_1 = (2\varepsilon_0 f^2/c b_0^2) E_c^2$). It can be seen from comparison with the curve

given in figure 4, built on the basis of experimental data, which is approximated by the straight line with the slope

$$\frac{\Delta_1}{E_c^2} = (11.0{-}13.5) \times 10^{-5}\ (\mathrm{m/MV})^2. \tag{5.11}$$

It should also be mentioned that the (formula (5.6)) value of the ratio $\varepsilon_0 a' f/c$ obtained above can be compared with the slope of the temperature dependence of parameter $\Delta_2 = \varepsilon_0 \tilde{\Delta}_2$ (determining the jump on the $\varepsilon_c'^{-1}(E_c^2)$ dependence); as follows from data, presented in figure 9,

$$\frac{\Delta_2}{T_c^0 - T} = \frac{2\varepsilon_0 a' f}{c} = (3.8{-}4.95) \times 10^{-4}\ \mathrm{K}^{-1}. \tag{5.12}$$

The estimates (5.6) and (5.12) practically coincide with each other.

Finally, using the formulae (5.6) and (5.10), we can estimate the ratio $f/a'b_0^2$ which determines the coefficient at E_c^2 in expression (4.5) for the transition temperature at nonzero field:

$$\frac{f}{a'b_0^2} = 0.274\ (\mathrm{m/MV})^2\ \mathrm{K}. \tag{5.13}$$

At the same time, according to the experimental data (figure 3) and to the formula (4.5) this ratio is equal to 0.27 $(\mathrm{m/MV})^2$.

On the whole, we see that the numerical estimates are sufficiently self-consistent. This fact confirms the validity of the basic assumptions about the character of temperature dependences and the signs of coefficients in the Landau expansion (4.1) for the free energy. The phase transition from the paraelectric to the ferroelectric phase remains of second order at $E_c \neq 0$. The transition takes place both due to the change of temperature and under the influence of the electric field E_c (in the range of temperatures $T \leqslant T_c^0$). The observed hysteresis phenomena on the field dependences of ε_c' can be related to the manifestations of the existence of the slightly nonequilibrium component of the internal field (polarization), which is overdamped to a great extent at $T \leqslant T_c$ due to ordering processes in the crystal.

6. Conclusions

Dielectric measurement of the dielectric permittivity of GPI crystal along the crystallographic c-axis has been done as a function of temperature and electric field. The electric field applied in the direction of the hydrogen-bonded phosphite anion chains causes a shift of the phase transition to lower temperatures (the critical temperature T_c decreases as E_c^2 starting from the initial value T_c^0). A dependence of permittivity ε_c' against field magnitude was observed both in the para- and ferroelectric phase. The jump-like changes of ε_c', which take place in the temperature region $T \leqslant T_c$ at certain field E_c values, correspond to the second order phase transition from the ferroelectric to the paraelectric phase. Above (far below) T_c^0 the permittivity ε_c' decreases (increases) with the field proportionally to E_c^2.

A symmetry analysis of the microscopic order parameter was performed. It was shown that the ferroelectric ordering along the b- (Y-) axis is accompanied by the antiferroelectric-like arrangement of the dipole moments in the direction (the c- (Z-) axis) of hydrogen bonded chains.

At the point of the phase transition induced by the electric field E_c, the rearrangement of protons on hydrogen bonds and the reversal of the corresponding dipole moments takes place. This results in the ferroelectric-like ordering of the dipole moment components along the c-axis and antiferroelectric-like ordering along the b-axis. Such an effect, which is achieved in a wide range of field values, is a manifestation of the high enough sensitivity of the proton

subsystem of the crystal with respect to the electric field acting along the H-bonded chains. It can be considered as a microscopic origin of the observed anomalously high values of the permittivity ε_c' [1] in the absence of an electric field at room temperature.

A thermodynamical analysis of the phase transition in the GPI crystal was performed on the basis of the Landau expansion written in terms of the two order parameters responsible for the dipole ordering along the *b*- and *c*-axes. On this basis the description of the observed dielectric anomalies is given. The numerical analysis performed shows that the results of theoretical consideration are in good agreement with the experimental data.

Acknowledgment

This work was partially supported by the Fundamental Researches Fund of the Ministry of Ukraine of Science and Education (Project No 02.07/00301).

Appendix

Starting from the Landau free energy expansion (4.1), and using the equilibrium conditions (4.4), we can obtain an expression for the entropy of the considered system

$$S = -\frac{\partial F}{\partial T} = S_0 - \frac{1}{2}a'\eta_b^2 - \frac{1}{2}b'\eta_c^2. \tag{A.1}$$

The contribution connected with the order parameters η_b and η_c are separated here. In the presence of the field E_c, as follows from the above-mentioned conditions,

$$\eta_b = 0, \qquad \eta_c = \frac{1}{b}E_c - \frac{d}{b^4}E_c^3 \tag{A.2}$$

in the paraelectric phase, and

$$\eta_b^2 = -\frac{1}{c}(a + f\eta_c^2), \qquad \eta_c = \frac{1}{\tilde{b}}E_c - \frac{\tilde{d}}{\tilde{b}^4}E_c^3 \tag{A.3}$$

in the ferroelectric phase (phase F), respectively. Being equal to zero above T_c, the η_b parameter can be interpreted as the 'true' one for the transition into phase F. The nonzero values of the parameter η_c are induced by the field E_c. Here and below we use an expansion in terms of E_c; the expressions (A.2) and (A.3) are written with an accuracy up to terms of the third order. For the entropy we have

$$S = S_0 - \frac{1}{2}\frac{b'}{b^2}E_c^2 + \frac{b'd}{b^5}E_c^4, \qquad T > T_c, \tag{A.4}$$

$$S = S_0 + \frac{1}{2}a'\frac{a}{c} + \frac{1}{2\tilde{b}^2}\left(\frac{fa'}{c} - b'\right)E_c^2 - \frac{\tilde{d}}{\tilde{b}^5}\left(\frac{fa'}{c} - b'\right)E_c^4, \qquad T < T_c. \tag{A.5}$$

The nonzero solution for η_b disappears at the temperature

$$T_c = T_c^0 - \frac{f}{a'b_0^2}E_c^2 + \frac{2f}{a'b_0^5}\left(d - \frac{b'f}{a'}\right)E_c^4 \tag{A.6}$$

which is the point of the phase transition at $E_c \neq 0$ (in addition to the formula (4.5); the terms of the fourth order are included in (A.6)).

It can be easily seen, taking into account the temperature dependence of coefficients a and b in the Landau expansion, that

$$S|_{T=T_c+0} = S|_{T=T_c-0} = S_0 - \frac{b'}{2b_0^2}E_c^2 + \frac{b'}{b_0^5}\left(d - \frac{b'f}{a'}\right)E_c^4. \tag{A.7}$$

The entropy is continuous at the transition point. At the same time, there exists a jump of specific heat C_E; the latter is determined by the relation

$$C_E = T\left(\frac{\partial S}{\partial T}\right)_E = -T\left(\frac{\partial^2 F}{\partial T^2}\right)_E. \tag{A.8}$$

In fact, using the expressions (A.4) and (A.5) we have

$$C_E|_{T=T_c+0} = C_E^0 + \frac{b'^2}{b^3}E_c^2 + \cdots, \tag{A.9}$$

$$C_E|_{T=T_c-0} = C_E^0 + T\frac{a'^2}{2c} + \frac{T}{b_0^3}\left(b' - \frac{fa'}{c}\right)E_c^2 + \cdots \tag{A.10}$$

and the value of jump ΔC_E follows from here immediately.

Such a behaviour of S and C_E is typical for the second order phase transition. The same conclusion can be made from the continuity of the order parameters η_b and η_c at the temperature T_c given by the expansion (A.6):

$$\eta_b|_{T\geqslant T_c} = 0, \qquad \eta_b|_{T<T_c} = \left[\frac{a'}{c}(T_c - T)\right]^{\frac{1}{2}}, \tag{A.11}$$

$$\eta_c|_{T=T_c+0} = \eta_c|_{T=T_c-0} = \frac{1}{b_0}E_c + \left(\frac{b'f}{a'} - d\right)\frac{f}{b_0^4}E_c^3. \tag{A.12}$$

Susceptibility along the ferroelectric b-axis

$$\chi_{yy} = \frac{1}{\varepsilon_0}\left(\frac{\partial^2 F}{\partial \eta_b^2}\right)^{-1} = \varepsilon_0^{-1}(a + 3c\eta_b^2 + f\eta_c^2)^{-1} \tag{A.13}$$

diverges at T_c; this divergency remains at the nonzero field E_c (at $T \geqslant T_c \chi_{yy} = \varepsilon_0^{-1}(a + f\eta_c^2)^{-1}$ and an equality to zero of the denominator of this expression coincides with the condition which determines T_c).

References

[1] Dacko S, Czapla Z, Baran J and Drozd M 1996 *Phys. Lett.* A **223** 217–20
[2] Baran J, Bator G, Jakubas R and Śledź M 1996 *J. Phys.: Condens. Matter* **8** 10647–58
[3] Averbuch-Pouchot M-T 1993 *Acta Crystallogr.* C **49** 815–8
[4] Shikanai F S, Komukae M, Czapla Z and Osaka T 2002 *J. Phys. Soc. Japan* **71** 498–503
[5] Taniguchi H, Machida M and Koyano N 2003 *J. Phys. Soc. Japan* **72** 1111–7
[6] Baran J, Śledź M, Jakubas R and Bator G 1997 *Phys. Rev.* B **55** 169–72
[7] Dacko S and Czapla Z 2000 *Ferroelectr. Lett.* **27** 17–21
[8] Shikanai F, Yamasaki M, Komukae M and Osaka T 2003 *J. Phys. Soc. Japan* **72** 325–9
[9] Tchukvinskyi B, Cach R, Czapla Z and Dacko S 1998 *Phys. Status Solidi* a **165** 309–16
[10] Yasuda N, Sakurai T and Czapla Z 1997 *J. Phys.: Condens. Matter* **9** L347–50
[11] Tchukvinski R, Czapla Z, Sobiestianskas R, Brilingas A, Grigas J and Baran J 1997 *Acta Phys. Pol.* A **92** 1191–6
[12] Sobiestianskas R, Brilingas A and Czapla Z 1998 *J. Korean Phys. Soc.* **32** S377–9
[13] Furtak J, Czapla Z and Kityk A V 1997 *Z. Naturf.* a **52** 778–82
[14] Okazaki K 1965 *Memoirs of the Defence Academy of Japan* vol 5, pp 99–108
[15] Lines M E and Glass A M 1997 *Principles and Applications of Ferroelectrics and Related Materials* (Oxford: Clarendon)
[16] Cach R and Dacko S 1989 *Acta Phys. Pol.* A **76** 521–27
[17] Stasyuk I, Czapla Z, Dacko S and Velychko O 2003 *Condens. Matter Phys.* **6** 483–98
[18] Stasyuk I V and Velychko O V 2001 *Phase Transit.* **73** 483–501